David Fulker
School of Mechanical and Manufacturing Engineering, University of New South Wales, Kensington Campus, Kensington, NSW 2025, Australia
e-mail: d.fulker@unsw.edu.au

Anne Simmons
School of Mechanical and Manufacturing Engineering, University of New South Wales, Kensington Campus, Kensington, NSW 2025, Australia
e-mail: a.simmons@unsw.edu.au

Tracie Barber
School of Mechanical and Manufacturing Engineering, University of New South Wales, Kensington Campus, Kensington, NSW 2025, Australia
e-mail: t.barber@unsw.edu.au

Computational Model of the Arterial and Venous Needle During Hemodialysis

Arteriovenous fistulae (AVF) are the favored choice of vascular access but still have poor long-term success. Hemodynamic parameters play an important role in vascular health and have been linked to the development of intimal hyperplasia (IH), a pathological growth of the blood vessel initiated by injury. This study aimed to investigate the hemodynamics surrounding the arterial needle (AN) and venous needle (VN), using computational fluid dynamics. A range of blood flow rates, needle positions, and needle orientations were examined. Disturbed flows were found around AN tip in both antegrade and retrograde orientations, which result in regions of high residency time on the surface of the vein and may disrupt endothelial function. Conversely, a high speed jet exits the VN, which produced high wall shear stresses (WSSs) at the point of impingement which can damage the endothelium. The secondary flows produced by jet dissipation also resulted in regions of high residency time, which may influence endothelial structure, leading to IH. The use of shallow needle angles, a blood flow rate of approximately 300 ml/min, and placement of the needle tip away from the walls of the vein mitigates this risk. [DOI: 10.1115/1.4034429]

Keywords: arterial needle, venous needle, hemodialysis, intimal hyperplasia

Introduction

The vascular access is a crucial component in renal replacement therapy as it allows blood to be extracted to the dialyzer. Arteriovenous fistulae (AVF) are the preferred choice of vascular access as they have a greater long-term success than grafts or catheter access [1]. Despite this, AVFs still have poor long-term success with 1 yr patency rates approximately 70%, declining to less than 48% within 4 yr of continual dialysis [2].

Thrombosis is the most common complication leading to vascular access failure and usually occurs under low flow conditions or when a stenotic lesion ruptures [3,4]. An effective treatment of thrombosis is to prevent the formation of a clinically significant stenosis. Stenosis commonly forms at the anastomosis, accounting for 50–70% of incidents, while stenosis at the venous outflow has the second highest number of incidents accounting for 20–50% of incidents [5,6]. Intimal hyperplasia (IH) is the pathological thickening of the blood vessel wall in response to injury and is the primary cause of stenosis formation in dialysis patients [7].

IH has been correlated with abnormal blood flows as the vascular endothelium has the ability to sense changes in wall shear stress (WSS). Blood vessels have been shown to maintain a physiological range of WSS to maintain homeostasis. Variations in flow resulting in low WSS [8], oscillatory WSS [9], or excessively high WSS [10,11] have been shown to induce "injury" to the endothelial layer, initiating the inflammatory pathway leading to IH. In particular, low WSS conditions stimulate vascular smooth muscle cell migration and proliferation [8], while oscillatory flows cause changes in the endothelial cell structure and orientation, which increases vascular permeability [12]. Residency time has become a prime indicator of intimal thickening as blood particles caught in low and oscillatory flows inevitably have a higher probability of interacting with the endothelial layer [13]. Conversely, exposure to high WSS in excess of 40 Pa can result in cell damage within 1 h [11], with extensive damage occurring if the WSS exceeds 150 Pa [14]. Prolonged exposure to impinging jets with high WSS can injure the blood vessel by denuding the endothelial layer resulting in intimal thickening from an inflammatory response [10].

The flow field surrounding hemodialysis needles is dynamic and has a direct influence on endothelial function. The venous needle jet (VNJ) produces a high level of mixing within the vein due to jet break down and entrainment of the core flow, with elevated turbulent intensities extending up to 8 cm downstream of the needle tip [15]. Huynh et al. [16] examined the effects of venous needle (VN) turbulence using cultured bovine aortic endothelial cells. It was shown that in the presence of the VNJ, endothelial cells were sheared off. Furthermore, turbulence produced by the needle flow resulted in a random alignment of endothelial cells and a decreased in nitric oxide production, a key mediator in vascular homeostasis. At the site of jet impingement, elevated levels of excessively high WSS are present [17], which have been shown to lead to endothelial denudation [10]. On the other hand, the arterial needle (AN) produces disturbed flows as the blood is extracted from the fistula [18]. Its design and position are fundamental in ensuring whether a large supply of blood is delivered to the dialyzer; however, the AN has remained unchanged.

It is hypothesized that flows produced by the hemodialysis needles may contribute to the high incidence of stenosis in the venous outflow. The present study uses computational fluid dynamics to assess the hemodynamic forces created by the AN and VN during hemodialysis. Metrics of WSS are employed to determine the extent of endothelial damage caused by the needles and to ascertain how cannulation technique may reduce the risk of potential IH.

Materials and Methods

Computational Model. An idealized model of the outflow vein from a radial–cephalic AVF was created using SolidWorks 2012 (Dassault systems, Velizy-Villacoublay, France). To investigate the full range of cannulated needle positions, a 15 gauge

Manuscript received June 5, 2016; final manuscript received August 1, 2016; published online November 4, 2016. Assoc. Editor: Tim David.

needle was placed at three angles (10 deg, 20 deg, and 30 deg), three depths (bottom, central, and top) and three blood flow rates (200 ml/min, 300 ml/min, and 400 ml/min). The VN was modeled in the antegrade orientation while the AN was modeled in both antegrade and retrograde orientations (conforming to current cannulation practice). The cephalic vein diameter is 10 mm (D) while the needle diameter is 1.35 mm (d) with a wall thickness of 0.18 mm. The needle was placed 100 mm ($10D$) upstream to ensure fully developed flow while a length of 200 mm ($40D$) was placed after the needle to allow sufficient development of the VNJ.

A fully structured hexahedral mesh was generated in ICEM CFD 14.5 (ANSYS, Inc., Canonsburg, PA). The boundary layer consisted of 40 layers with an initial size of 0.02 mm and a growth rate of 1.05 and a total of 8×10^6 elements in the entire domain. Steady flow conditions were simulated in the grid convergence tests. Velocity fluctuations due to poor spatial resolution were minimized to within 1% when the mesh size exceeded 8×10^6 elements. The boundary layer was also assessed using the grid convergence index as outlined by Roache [19]. The maximum WSS within the vein produced by the impinging VNJ was measured on mesh sizes of 1, 2, 4, 8, and 16×10^6 elements. A boundary layer consisting of 40 prismatic layers yielded a difference in the maximum WSS of 3.1%, confirming grid independence to a high accuracy. Stereo particle image velocimetry data was previously collected on a scaled model of the cannulation setup. The average maximum and mean velocity variations from velocity profiles are displayed in Table 1, ensuring validity in the simulations.

The Navier–Stokes equations were solved using Fluent 14.5 (Fluent, Inc., Lebanon, NH). A laminar model was employed with a pressure-implicit with splitting of operators (PISO) algorithm for the pressure–velocity coupling and spatial discretization schemes set to bounded central differencing to stabilize the dissipation of the VNJ. The walls of the vein and needle were assumed to be rigid and smooth as the vein wall thickens from arterialization during the maturation process after the fistula is created. Blood was modeled as a Newtonian fluid with a density of 1045 kg/m^3 and a viscosity of 0.0035 Pa·s. The VN was modeled with a constant parabolic velocity inlet with Reynolds numbers of 924, 1385, and 1847 for flow rates of 200 ml/min, 300 ml/min, and 400 ml/min, respectively. The AN was modeled with a pulsatile waveform incorporating the effects of the hemodialysis roller pump as described in a previous study [20]. The AN waveform has a period of 0.64 s with equivalent average Reynolds numbers as previously mentioned. A zero pressure opening was imposed downstream to meet flow continuity. A transient waveform with a period of 1 s as measured by Sivanesan et al. [21] was enforced at the cephalic vein inlet. The resultant Womersley number of the cephalic vein waveform was 2.8 and the maximum, minimum, and mean Reynolds numbers are 930, 225, and 553, respectively.

The domain was initialized for ten periods of the transient profile with a time step of 0.01 s to allow the flow fields produced by the vein and needle to stabilize. To reduce velocity fluctuations induced by inadequate time resolution, the time step was then reduced to 0.0001 s ensuring the average Courant number remained below one. All residual errors converged to 10^{-6} within five iterations. Furthermore, a time step of 0.0001 s concurs with the high-resolution CFD recommendations of Khan et al. [22], who concluded that at least 10,000 time steps per cardiac cycle are required in order to sufficiently resolve complex hemodynamic flows.

Table 1 Variation between simulations and experimental data

Needle	Percentage difference in maximum velocity	Percentage difference in mean velocity
Arterial antegrade	8.28	15.23
Arterial retrograde	5.68	4.48
Venous	17.86	20.78

Metric Analysis. Two WSS metrics are employed in this study to analyze potential endothelial dysfunction: time average WSS (TAWSS) and relative residency time (RRT). TAWSS is used to assess excessively high WSS produced by the VNJ, which occurs over the cardiac cycle and is defined as

$$\text{TAWSS} = \frac{1}{T}\int_0^T |\boldsymbol{\tau_w}|\ dt$$

where T is the period of the cardiac cycle and τ_w is the instantaneous WSS vector. RRT was proposed by Himburg et al. [13] and is sensitive to both the direction and magnitude of the WSS vector. The RRT represents the relative time a particle near the wall will travel in one cardiac cycle and is defined as

$$\text{RRT} = \frac{\mu}{T}[(1 - 2 * \text{OSI}) * \text{TAWSS}]^{-1}$$

where μ is the dynamic viscosity and oscillatory shear index (OSI) is the oscillatory shear index (OSI) introduced by He and Ku [23]. This study utilizes the RRT as a single metric for low and oscillating WSS, as previous studies have noted its robustness [24] and accuracy [25] in predicting intimal thickening. These metrics were calculated over ten cardiac cycles to sufficiently represent the time averaged affects occurring over a dialysis session. The area of high WSS and RRT was calculated using the average cell area and summing the total number of the cells (j) above the maximum threshold, formulated as

$$A_{>\text{threshold}} = \sum_{i=1}^{j} N_{>\text{threshold}} * A_{\text{average}}$$

where $A_{>\text{threshold}}$ is the vein area larger than the threshold value (40 Pa), which can cause endothelial damage, $N_{>\text{threshold}}$ is the number of cells above the set threshold value, and A_{average} is the average cell area.

Results

Arterial Needle Antegrade. Figure 1 displays velocity contours and streamlines on cross-sectional planes for the AN placed in the antegrade orientation. In all cases, the blood being drawn through the needle is localized around the needle tip and a disturbed flow region exists directly above the central bore. The disturbed flow region consists of blood being extracted through the needle and its size remained consistent for all cases except when the needle tip was placed closer to the vein wall. In these positions, the wall influenced the size of the disturbed flow region occurring above the needle tip, where a needle placed near the floor resulted in a larger disturbed flow region while a needle placed near the roof had a smaller disturbed flow region. Disturbed flow downstream of the needle tip along the floor of the vein also formed at high blood flow rates, shallow needle angles, and when the needle tip was placed toward the roof of the vein, although the disturbed flow that formed on the floor of the vein was not drawn into the AN.

The RRT on the surface of the vein is presented in Fig. 2, with higher residency times coinciding with the location of the disturbed flows identified previously. The isometric view of the blood vessel highlights the three-dimensional nature of the disturbed flows, as high residency times extend from the roof of the vein to the side walls. A higher blood flow rate increases the strength of the disturbed flows, while a variation of the needle angle and depth shifts the position of high residency times within the vein. Figure 1 showed that the needle disrupts the flow downstream; however,

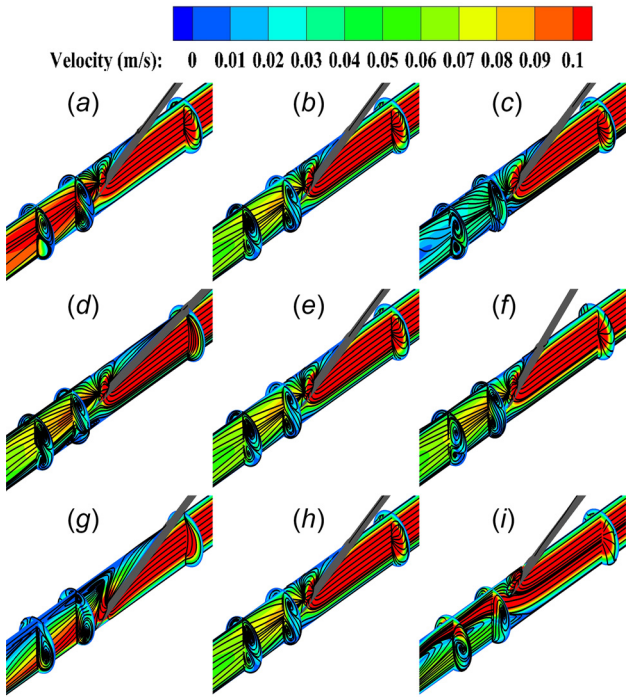

Fig. 1 Pathlines and velocity contours on cross-sectional planes for the arterial needle in an antegrade orientation during diastole. (*a*)–(*c*) Variation in blood flow rate (200 ml/min, 300 ml/min, 400 ml/min). (*d*)–(*f*) Variation in needle angle (10 deg, 20 deg, 30 deg). (*g*)–(*i*) Variation in needle position (bottom, central, top).

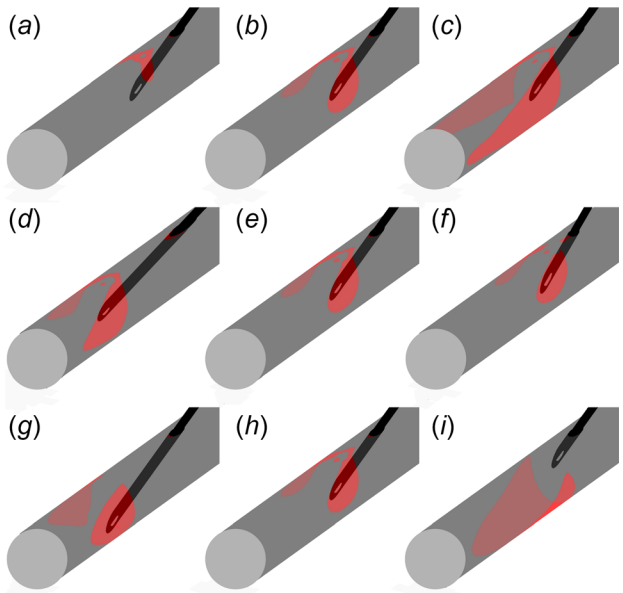

Fig. 2 Relative residency time on the wall of the vein normalized by the mean wall shear stress for the arterial needle in the antegrade orientation. Low levels of high RRT (<10) have been highlighted to emphasize regions of strong secondary flows. (*a*)–(*c*) Variation in blood flow rate (200 ml/min, 300 ml/min, 400 ml/min). (*d*)–(*f*) Variation in needle angle (10 deg, 20 deg, 30 deg). (*g*)–(*i*) Variation in needle position (bottom, central, top).

these disturbed flows do not have high residency times except when the needle is placed near the roof of the vein.

The area of high RRT for the AN in antegrade is summarized in Table 2. Smaller regions were produced at lower blood flow rates,

Table 2 Summary of back eye flow and area of high RRT for all tested parameters of the arterial needle in the antegrade orientation

Parameter	Back eye flow (%)	Area of high RRT (cm^2)
200 ml/min	44	3.98
300 ml/min	42	45.01
400 ml/min	41	122.51
10 deg	41	38.04
20 deg	42	45.01
30 deg	43	50.06
Needle at bottom of vein	33	43.67
Needle at center of vein	42	45.01
Needle at top of vein	48	68.64

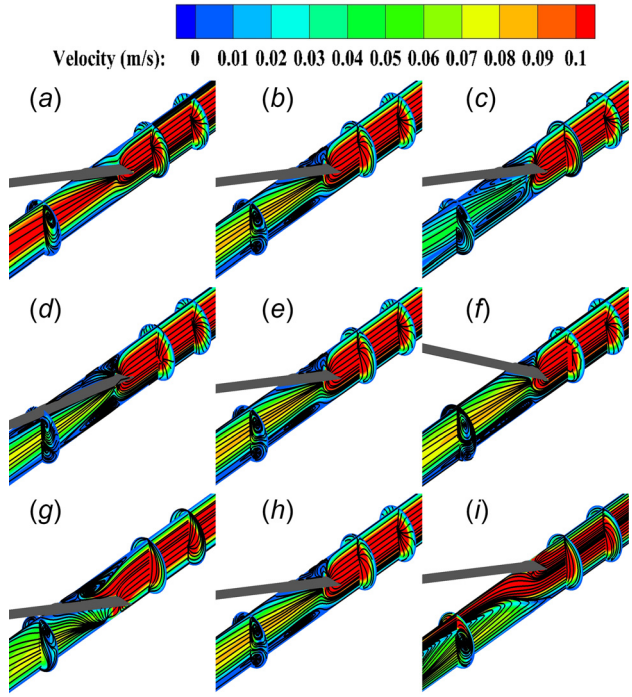

Fig. 3 Pathlines and velocity contours on cross-sectional planes for the arterial needle in a retrograde orientation during diastole. (*a*)–(*c*) Variation in blood flow rate (200 ml/min, 300 ml/min, 400 ml/min). (*d*)–(*f*) Variation in needle angle (10 deg, 20 deg, 30 deg). (*g*)–(*i*) Variation in needle position (bottom, central, top).

while the largest affected area occurred at blood flow rates of 400 ml/min. The severity of the affected area also increased with greater needle angles and a needle is placed near the roof of the vein. Table 2 also summarizes the amount of blood entering the back eye. The amount of flow entering the back eye remained fairly constant in all cases except when the needle position was varied. A needle placed toward the roof of the vein resulted in the highest amount of blood entering the needle.

Arterial Needle Retrograde. Velocity contours and pathlines on cross-sectional planes for the AN placed in the retrograde orientation are displayed in Fig. 3. In this orientation, the region of core flow being entrained by the needle is much smaller than the antegrade orientation. A disturbed flow region occurs above the needle tip and is primarily located around the needle insertion site. Disturbed flows also occur below the needle in all cases except at blood flow rates of 200 ml/min. The needle position and blood flow rate have a strong influence on the size of the disturbed flow regions.

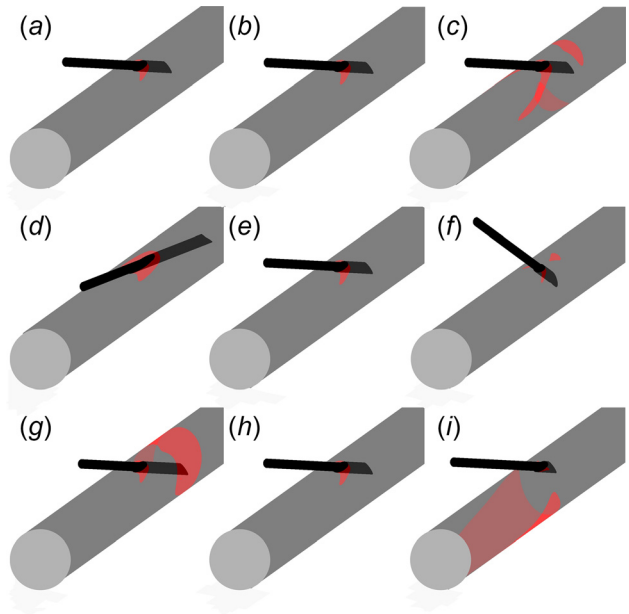

Fig. 4 Relative residency time on the wall of the vein normalized by the mean wall shear stress for the arterial needle in the retrograde orientation. Low levels of high RRT (<10) have been highlighted to emphasize regions of strong secondary flows. (*a*)–(*c*) Variation in blood flow rate (200 ml/min, 300 ml/min, 400 ml/min). (*d*)–(*f*) Variation in needle angle (10 deg, 20 deg, 30 deg). (*g*)–(*i*) Variation in needle position (bottom, central, top).

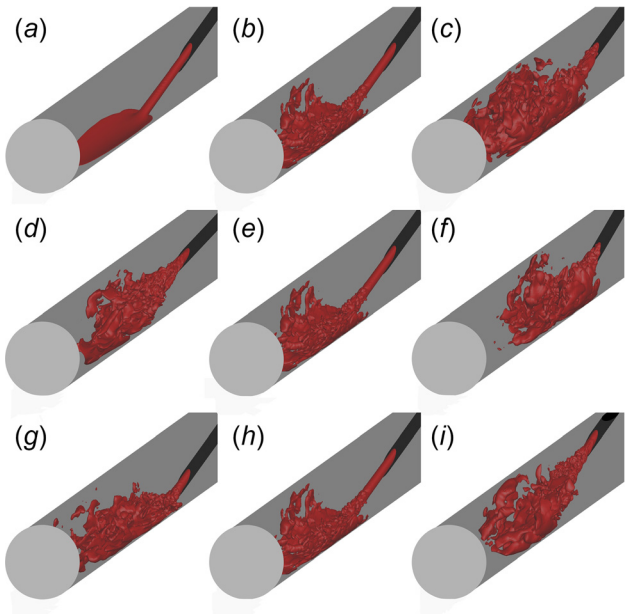

Fig. 5 Velocity isosurfaces (1 m/s) visualizing the venous needle jet. (*a*)–(*c*) Variation in blood flow rate (200 ml/min, 300 ml/min, 400 ml/min). (*d*)–(*f*) Variation in needle angle (10 deg, 20 deg, 30 deg). (*g*)–(*i*) Variation in needle position (bottom, central, top).

Table 3 Summary of back eye flow and area of high RRT for all tested parameters of the arterial needle in the retrograde orientation

Parameter	Back eye flow (%)	Area of high RRT (cm^2)
200 ml/min	35	1.82
300 ml/min	37	2.36
400 ml/min	37	12.90
10 deg	37	1.66
20 deg	37	2.36
30 deg	36	3.00
Needle at bottom of vein	39	55.40
Needle at center of vein	37	2.36
Needle at top of vein	37	6.98

Figure 4 displays the RRT on the surface of the vein for the AN in the retrograde orientation. Regions of high residency time coincide with the locations of the disturbed flows displayed in Fig. 3. High blood flow rates increased the area of high residency time; however, the position of the needle tip with respect to the vein wall had the greatest influence.

Table 3 displays the area of high RRT and amount of blood entering the back eye for the AN in retrograde orientation. A retrograde orientation displayed smaller areas of high RRT compared to an antegrade orientation in all cases except for a needle placed near the bottom of the vein. Similar trends were exhibited where higher blood flow rates and greater needle angles increased residency times, although the effect of needle angle was minimal. A needle placed near the floor of the vein or with a blood flow rate of 400 ml/min yielded the largest areas. The amount of blood entering the back eye for a retrograde placed AN remained relatively similar for all blood flow rates and needle positions. The level of back eye flow was also lower in all cases compared to the antegrade orientation except for a needle placed near the floor of the vein.

Table 4 Summary of back eye flow and area of high RRT for all tested parameters of the venous needle

Parameter	Back eye flow (%)	Area of high RRT (cm^2)	Area of high (>40 Pa) TAWSS (cm^2)
200 ml/min	0.43	4.39	7.02
300 ml/min	0.29	3.73	9.92
400 ml/min	0.25	4.69	14.65
10 deg	0.07	1.31	0
20 deg	0.29	3.73	9.92
30 deg	1.99	6.13	15.06
Needle at bottom of vein	0.44	0.79	28.21
Needle at center of vein	0.29	3.73	9.92
Needle at top of vein	0.27	8.97	0.10

Venous Needle. The structure of the VNJ and subsequent mixing are displayed in Fig. 5. At blood flow rates of 200 ml/min and 300 ml/min, the exiting jet structure is coherent and laminar. The jet begins to break down as it approaches the vein, which indicates that information is translated upstream as the jet approaches the vein floor. Upon impingement on the floor of the vein, the jet begins to spread and secondary flows develop, followed by complex mixing. Secondary flows are exhibited in every case except at lower blood flow rates. At blood flow rates of 400 ml/min, jet dissipation occurs directly after exiting the needle. The angle of the needle has little influence on the exiting jet structure and downstream mixing.

Table 4 shows that the flow exiting the VN back eye is minimal in every case, where the exiting jet structure is not influenced by the presence of the back eye in the VN. The percentage rises slightly when the needle is inserted at 30 deg.

The effects of excessively high TAWSS are displayed in Fig. 6. In all cases except at shallow needle angles, a large region of high TAWSS occurs at the point of jet impingement. Table 4 also displays the area of TAWSS above 40 Pa. High blood flow rates and greater needle angles increase the area of excessively high TAWSS; however, the greatest force is produced when the needle tip is placed closest to the floor of the vein.

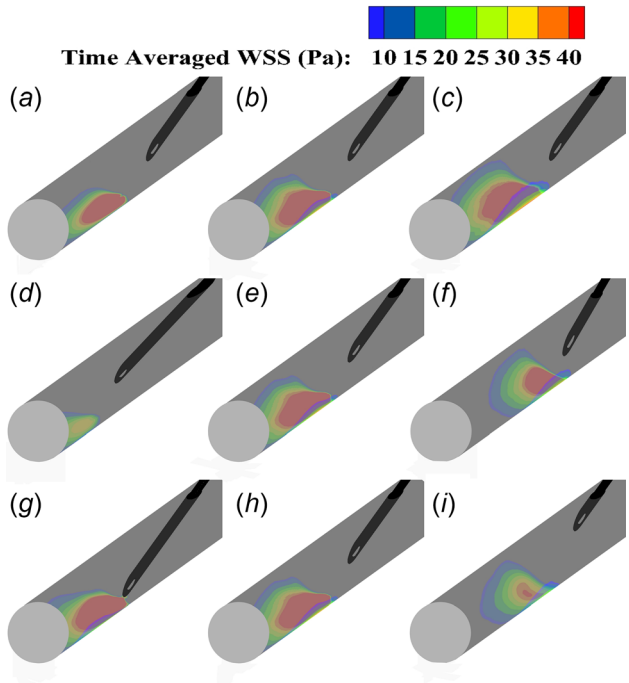

Fig. 6 Time average wall shear stress on the wall of the vein for the venous needle. Values < 10 Pa have been highlighted to emphasize regions of excessively high stress. The scale has also been capped at the threshold reported to cause endothelial damage (40 Pa). (*a*)–(*c*) Variation in blood flow rate (200 ml/min, 300 ml/min, 400 ml/min). (*d*)–(*f*) Variation in needle angle (10 deg, 20 deg, 30 deg). (*g*)–(*i*) Variation in needle position (bottom, central, top).

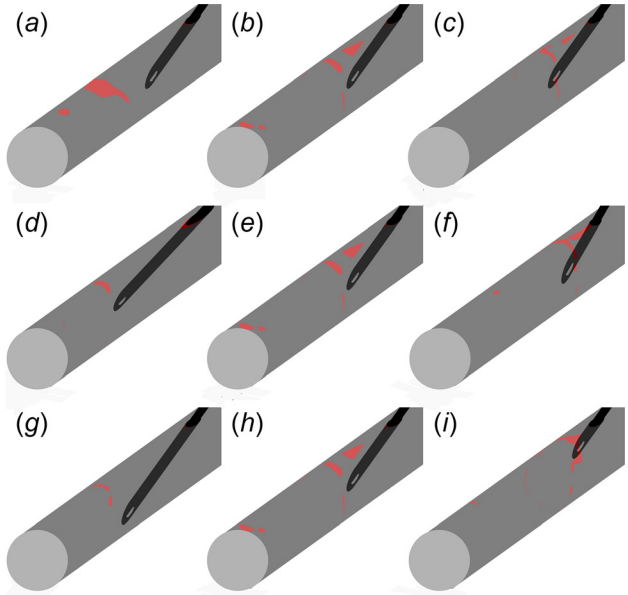

Fig. 7 Relative residency time on the wall of the vein normalized by the mean wall shear stress for the arterial needle in the retrograde orientation. Low levels of high RRT (<10) have been highlighted to emphasize regions of strong secondary flows. (*a*)–(*c*) Variation in blood flow rate (200 ml/min, 300 ml/min, 400 ml/min). (*d*)–(*f*) Variation in needle angle (10 deg, 20 deg, 30 deg). (*g*)–(*i*) Variation in needle position (bottom, central, top).

Figure 7 displays the RRT on the vein surface and indicates that pockets of the secondary flows contain low and oscillating WSS. Patches of high residency time appear on the roof of the vein above the needle tip and downstream, in the region where secondary flows are present after jet impingement. The area of high RRT is presented in Table 4 and shows that high (400 ml/min) and low (200 ml/min) blood flow rates as well as sharp needle angles produce regions of higher residency times, while a needle placed near the roof of the vein produces the largest area.

Discussion

Dialysis needles may influence the formation of IH and may contribute to the high incidence of stenotic lesions, which develop in the venous outflow of AVFs. Stenotic lesions often lead to thrombosis, the primary reason of reduced patency in vascular access, due to reduced flow conditions or lesion rupture [3,25]. Stenosis due to IH develops as a response to endothelial injury and has a high correlation with blood flows, in particular low WSS [8], oscillatory WSS [9], or excessively high WSS [10,11].

Arterial Needle. Results for the AN in an antegrade and retrograde orientation demonstrated strong secondary flows localized around the needle tip, as the blood was withdrawn from the vein. In the antegrade orientation, the flow must travel around the needle before being entrained through the central bore. The disturbed flow region is created from reduced flow produced by the drag force of the needle. Its size and strength are therefore highly dependent on the position of the needle within the vein. This was most clearly demonstrated when the needle was placed close to the vein floor, resulting in the strongest disturbed flows. Another disturbed flow region also formed along the floor of the vein at high blood flow rates and shallow needle angles and was most pronounced when the needle tip was placed toward the roof of the vein. The risk of access recirculation may be higher when the needle is in these positions. Rothera et al. [26] examined the influence of needle separation distance on access recirculation and found that needles placed within 2.5 cm of each other do not result in access recirculation, which is similar to the results found in our study where secondary flows did not extend further than 2.5 cm. Ultrasound guides may be used to optimize the needle position within the blood vessel to minimize potential access recirculation and the risk of intimal thickening, which is prone to developing in disturbed flows. The region of core flow being entrained in the retrograde orientation is much smaller compared to the antegrade orientation. In this orientation, the disturbed flow region was located around the needle tip and insertion site due to the drag forces imposed by the needle body, which retards the flow. A larger disturbed flow region also formed below the needle which may contribute to access recirculation. However, this only extended a few centimeters downstream indicating that the risk of access recirculation is not dependant on AN orientation. Ozmen et al. [27] also reported no statistical difference in access recirculation between antegrade and retrograde orientation.

Endothelial cells are sensitive to flow reversal and oscillating flows as these flows change the structure of the endothelial layer from regular striated patterns to random orientations, which increases vascular permeability and endothelial cell turnover, leaving the blood vessel susceptible to deposition of inflammatory mediators [12,28]. The strong secondary flows around the AN coincided with regions of high residency time, which may lead to IH. For the antegrade orientation, they extend from the roof of the vein to the side walls while the retrograde orientation showed localized areas around the insertion site and floor of the vein. The localization of high residency time flows may have a direct impact on vascular patency as the insertion site forms a direct pathway to transport inflammatory mediators into the underlying layers of the vascular wall. Aneurysms commonly form at the needle insertion sites due to a weakened blood vessel from repeated needle puncture [29]. The localization of disturbed flows around the insertion site may be a contributing factor to this complication.

For both needle orientations, the blood flow rate had the greatest influence on the area affected by high RRT, where higher flows coincided with a larger region of RRT. The position of the needle shifted the affected region, with the greatest reduction evident when the needle tip was located in the center of the vein at a shallow angle, away from the walls of the blood vessel. For an AN in antegrade or retrograde orientation, the results of this study suggest that the optimum method to reduce the risk of IH is to use lower blood flow rates. However, it is noted that this can require longer dialysis sessions to attain the required clearance, which may conflict with the patient's lifestyle. Ensuring the needle tip is placed away from the walls of the blood vessel may also reduce the risk of intimal thickening. While this study found larger regions of RRT with an antegrade orientation indicating an increased risk of IH, Parisotto et al. [30] reported an 18% increase in risk of access failure with the retrograde orientation. Access failure can occur from a range of factors such as infection or aneurysm blow out. The higher access failure of retrograde orientation has been attributed to the endothelial flap which is created with retrograde puncture, which may be held open through fistula flow forces after the needle is removed.

For the antegrade orientation, the amount of blood entering the back eye remained consistent, between 41% and 44% for all needle angles and blood flow rates. Needle depth had the greatest influence on back eye flow due to the resistance imposed by the walls of the blood vessel. The amount of flow entering the back eye was lower in the retrograde orientation than antegrade orientation, remaining consistently between 35% and 39% for all needle positions and blood flow rates. This result is explained through the position of the back eye, whose role is to reduce the resistance in the central bore. In the retrograde orientation, the path of least resistance for the core flow is directly through the central bore due to the direction of needle placement. This study indicates that needle orientation influences the resistance of flow entering the AN, where an antegrade orientation may increase the negative pressure in the arterial line due to higher back eye efficiency.

Venous Needle. A high speed jet was shown to exit the VN. Upon impingement on the vein floor, the jet begins to spread and creates complex secondary flows. These complex secondary flows were examined in every case except at blood flow rates of 200 ml/min. The jet is coherent and laminar at lower blood flow rates but unstable at 400 ml/min. The potential core of all jets does not contain turbulent mixing and maintains a constant velocity [31], which explains the coherent structure seen in most cases. At higher blood flow rates, the length of the potential core is reduced and the flow exiting the central bore becomes transitional as seen at blood flow rates of 400 ml/min. The increase in jet dissipation which occurs close to the impingement zone is due to a rise in static pressure near the wall following the decrease in momentum [32]. The effects of the wall are subsequently translated upstream through the jet, triggering early jet break down. The minimal flow through the back eye shows that this feature has very little influence on the exiting jet structure. The slight rise in back eye flow when the needle was placed at 30 deg can be attributed to the increased exposure to the core flow.

Elevated level of TAWSS (above the threshold reported to denude the endothelium) was identified at the impingement zone. The region of high TAWSS is caused by the translation of momentum upon impingement. Higher blood flow rates, greater needle angles, and a needle tip placed closer to the vein floor produced larger regions of elevated TAWSS. In these cases, the velocity of the jet is higher or the effects of dissipation are constrained, as the jet travels a shorter distance resulting in a greater force upon impingement. High WSS has been shown by others at lower jet heights and higher jet Reynolds numbers on jet impingement on a flat plate at normal incidence [31]. Only a shallow needle angle prevented a region of high TAWSS, as the jet is provided a longer distance before impingement, providing greater dissipation which reduces the velocity of the jet. Therefore, lower blood flow rates, shallow needle angles, and placement of the needle tip away from the floor of the vein can reduce the high TAWSS occurring at the point of jet impingement.

Conversely, regions of high RRT were found on the roof of the vein downstream of the needle tip, which coincided with the secondary flows produced by jet break down. This indicates that steady secondary flows occur in the disturbed flow regions, which result in high residency times. High RRT can stimulate vascular smooth muscle cell migration and proliferation [8] and increases vascular permeability [12], potentially leading to IH [25]. Similar regions of high RRT were found at blood flow rates of 200 ml/min and 400 ml/min, indicating that low blood flow rates produce steady secondary flows while high blood flow rates produce more pockets of complex secondary flows. This is linked to the transitional flow in the VN, where Reynolds numbers range between 924 and 1847, indicating that an optimum blood flow rate exists which can minimize RRT. Ponce et al. [33] showed patients were at a significantly higher risk of AVF failure at blood flow rates below 310 ml/min and greater than 400 ml/min. Sharp needle angles and a needle tip placed near the roof of the vein also produced regions of higher residency time as these parameters influenced the production of secondary flows. Therefore, a blood flow rate around 300 ml/min, shallow needle angles, and placement of the needle tip away from the roof of the vein may minimize the risk of IH.

Influence of the Needles. The influence of the needles can be examined in cases where cannulation is not conducted, such as animal models of fistulae and in patients who received a kidney transplant whose fistula was not tied off. Patard et al. [34] examined fistulas which remained open after kidney transplant and found that only 17.5% of AVFs thrombosed, over a mean time of 39 months representing a 4 yr patency rate of 61%. Similar results have been reported in other studies over comparable time frames [5]. These figures compare favorably to the 48% 4-yr patency rate found by Kazemzadeh et al. [2], indicating that the needles influence the development of vascular complications. However, Wang et al. [6] identified intimal thickening in the proximal vein of pig AVFs within 42 days of surgery, showing that other factors stimulate the development of IH.

Regions of high TAWSS and RRT were found downstream of the VN while disturbed flow regions with high RRT surround the AN, which may contribute to endothelial damage and IH. Glashan and Walker [35] examined vein samples in hemodialysis fistulas and found endothelial damage and loss in the vicinity of the needle tip. However, stenosis commonly forms at the anastomosis in AVFs [21,36], despite the high potential of endothelial damage near the needles. This suggests that endothelial recovery plays an important role in vascular health. Reidy and Schwartz [37] used rats to study denudation and recovery by removing endothelial cells in the aorta. Reendothelialization through migration and proliferation was complete after 2–4 days, highlighting the ability of the blood vessel to recover. Endothelial denudation has been shown to lead to intimal lesions if the period of denudation continues for several days [38].The time frames of recovery are significant as hemodialysis sessions are usually conducted every 2–4 days, indicating that the blood vessel may recover from any damage caused by the needles, thus explaining why stenosis more frequently form at the anastomosis.

Conclusion

Regions of high residency time corresponding to areas of disturbed flow were examined on the vein wall for both needles. High TAWSS, above the threshold reported to cause endothelial damage, was also measured downstream of the VN coinciding with the point of VNJ impingement. These regions of high residency time and high TAWSS indicate potential sites of endothelial dysfunction which may lead to IH. The use of shallow needle

angles, a blood flow rate of approximately 300 ml/min, and placement of the needle tip away from the walls of the vein mitigates this risk.

References

[1] Levey, A. S., Coresh, J., Balk, E., Kausz, A. T., Levin, A., Steffes, M. W., Hogg, R. J., Perrone, R. D., Lau, J., and Eknoyan, G., 2003, "National Kidney Foundation Practice Guidelines for Chronic Kidney Disease: Evaluation, Classification, and Stratification," Ann. Intern. Med., **139**(2), pp. 137–147.

[2] Kazemzadeh, G. H., Modaghegh, M.-H. S., Ravari, H., Daliri, M. R., Hoseini, L., and Nateghi, M. R., 2012, "Primary Patency Rate of Native AV Fistula: Long Term Follow Up," Int. J. Clin. Exp. Med., **5**(2), pp. 173–178.

[3] Van Tricht, I., De Wachter, D., Tordoir, J. H. M., and Verdonck, P., 2005, "Hemodynamics and Complications Encountered With Arteriovenous Fistulas and Grafts as Vascular Access for Hemodialysis: A Review," Ann. Biomed. Eng., **33**(9), pp. 1142–1157.

[4] Kaushal, K., and Wilson, S. E., 2010, "Thrombophilia as a Cause of Recurrent Vascular Access Thrombosis in Hemodialysis Patients," *Vascular Access: Principles and Practice*, Lippincott Williams & Wilkins, Philadelphia, PA, pp. 44–47.

[5] Trampuz, B. V., Ponikvar, R., Kandus, A., and Ponikvar, J. B., 2013, "Hemodialysis Arteriovenous Fistula-Related Complications and Surgery in Kidney Graft Recipients," Ther. Apheresis Dial., **17**(4), pp. 444–447.

[6] Wang, Y., Krishnamoorthy, M., Banerjee, R., Zhang, J., Rudich, S., Holland, C., Arend, L., and Chaudhury, P. R., 2008, "Venous Stenosis in a Pig Arteriovenous Fistula Model—Anatomy, Mechanisms and Cellular Phenotypes," Nephrol. Dial. Transplant., **23**(2), pp. 525–533.

[7] Nassar, G. M., Rhee, E., Khan, A. J., Nguyen, B., Achkar, K., and Beathard, G., 2015, "Percutaneous Thrombectomy of AVF: Immediate Success and Long-Term Patency Rates," Semin. Dial., **28**(2), pp. 15–22.

[8] Meyerson, S. L., Skelly, C. L., Curi, M. A., Shakur, U. M., Vosicky, J. E., Glagov, S., and Schwartz, L. B., 2001, "The Effects of Extremely Low Shear Stress on Cellular Proliferation and Neointimal Thickening in the Failing Bypass Graft," J. Vasc. Surg., **34**(1), pp. 90–97.

[9] Keynton, R. S., Evancho, M. M., Sims, R. L., Rodway, N. V., Gobin, A., and Rittgers, S. E., 2001, "Intimal Hyperplasia and Wall Shear in Arterial Bypass Graft Distal Anastomoses: An In Vivo Model Study," ASME J. Biomech. Eng., **123**(5), pp. 464–473.

[10] Vaishnav, R. N., Patel, D. J., Atabek, B. H., Deshpande, M. D., Plowman, F., and Vossoughi, J., 1983, "Determination of the Local Erosion Stress of the Canine Endothelium Using a Jet Impingement Method," ASME J. Biomech. Eng., **105**(1), pp. 77–83.

[11] Fry, D. L., 1968, "Acute Vascular Endothelial Changes Associated With Increased Blood Velocity Gradients," Circ. Res., **22**(2), pp. 165–197.

[12] Chien, S., 2008, "Effects of Disturbed Flow on Endothelial Cells," Ann. Biomed. Eng., **36**(4), pp. 554–562.

[13] Himburg, H. A., Grzybowski, D. M., Hazel, A. L., LaMack, J. A., Li, X.-M., and Friedman, M. H., 2004, "Spatial Comparison Between Wall Shear Stress Measures and Porcine Arterial Endothelial Permeability," Am. J. Physiol.: Heart Circ. Physiol., **286**(5), pp. H1916–1922.

[14] Leverett, B. L., Hellums, D. J., Alfrey, C. P., and Lynch, E. C., 1972, "Red Blood Cell Damage by Shear Stress," Biophys. J., **12**(3), pp. 257–273.

[15] Unnikrishnan, S., Huynh, T. N., Brott, B. C., Ito, Y., Cheng, C.-H., Shih, A. M., Allon, M., and Anayiotos, A. S., 2005, "Turbulent Flow Evaluation of the Venous Needle During Hemodialysis," ASME J. Biomech. Eng., **127**(7), pp. 1141–1146.

[16] Huynh, T. N., Chacko, B. K., Teng, X., Brott, B. C., Allon, M., Kelpke, S. S., Thompson, J. A., Patel, R. P., and Anayiotos, A. S., 2007, "Effects of Venous Needle Turbulence During Ex Vivo Hemodialysis on Endothelial Morphology and Nitric Oxide Formation," J. Biomech., **40**(10), pp. 2158–2166.

[17] Fulker, D., Kang, M., Simmons, A., and Barber, T., 2013, "The Flow Field Near a Venous Needle in Hemodialysis: A Computational Study," Hemodialysis Int., **17**(4), pp. 602–611.

[18] Fulker, D., Simmons, A., Kabir, K., Kark, L., and Barber, T., 2015, "The Hemodynamic Effects of Hemodialysis Needle Rotation and Orientation in an Idealized Computational Model," Artif. Organs, **40**(2), pp. 185–189.

[19] Roache, P. J., 1997, "Quantification of Uncertainty in Computational Fluid Dynamics," Annu. Rev. Fluid Mech., **29**(1), pp. 123–160.

[20] Fulker, D., Keshavarzi, G., Simmons, A., Pugh, D., and Barber, T., 2015, "Pulsatility Produced by the Hemodialysis Roller Pump as Measured by Doppler Ultrasound," Artif. Organs, **39**(11), pp. 945–950.

[21] Sivanesan, S., How, T. V., Black, R. A., and Bakran, A., 1999, "Flow Patterns in the Radiocephalic Arteriovenous Fistula: An In Vitro Study," J. Biomech., **32**(9), pp. 915–925.

[22] Khan, M. O., Valen-Sendstad, K., and Steinman, D. A., 2015, "Narrowing the Expertise Gap for Predicting Intracranial Aneurysm Hemodynamics: Impact of Solver Numerics Versus Mesh and Time-Step Resolution," Am. J. Neuroradiology, **36**(7), pp. 1310–1316.

[23] He, X., and Ku, D. N., 1996, "Pulsatile Flow in the Human Left Coronary Artery Bifurcation: Average Conditions," ASME J. Biomech. Eng., **118**(1), pp. 74–82.

[24] Lee, S.-W., Antiga, L., and Steinman, D. A., 2009, "Correlations Among Indicators of Disturbed Flow at the Normal Carotid Bifurcation," ASME J. Biomech. Eng., **131**(6), p. 061013.

[25] Knight, J., Olgac, U., Saur, S. C., Poulikakos, D., Marshall, W., Cattin, P. C., Alkadhi, H., and Kurtcuoglu, V., 2010, "Choosing the Optimal Wall Shear Parameter for the Prediction of Plaque Location—A Patient-Specific Computational Study in Human Right Coronary Arteries," Atherosclerosis, **211**(2), pp. 445–450.

[26] Rothera, C., McCallum, C., Huang, S., Heidenheim, P., and Lindsay, R., 2011, "The Influence of Between-Needle Cannulation Distance on the Efficacy of Hemodialysis Treatments," Haemodialysis Int., **15**(4), pp. 546–552.

[27] Ozmen, S., Kadiroglu, A. K., Ozmen, C. A., Danis, R., Sit, D., Akin, D., and Yilmaz, M. E., 2008, "Does the Direction of Arterial Needle in AV Fistula Cannulation Affect Dialysis Adequacy?," Clin. Nephrol., **70**(3), pp. 229–232.

[28] Bassiouny, H. S., White, S., Glagov, S., Choi, E., Giddens, D. P., and Zarins, C. K., 1992, "Anastomotic Intimal Hyperplasia: Mechanical Injury or Flow Induced," J. Vasc. Surg., **15**(4), pp. 708–717.

[29] van Loon, M. M., Goovaerts, T., Kessels, A. G. H., van der Sande, F. M., and Tordoir, J. H. M., 2010, "Buttonhole Needling of Haemodialysis Arteriovenous Fistulae Results in Less Complications and Interventions Compared to the Rope-Ladder Technique," Nephrol., Dial., Transplant., **25**(1), pp. 225–230.

[30] Parisotto, M. T., Schoder, V. U., Miriunis, C., Grassmann, A. H., Scatizzi, L. P., Kaufmann, P., Stopper, A., and Marcelli, D., 2014, "Cannulation Technique Influences Arteriovenous Fistula and Graft Survival," Kidney Int., **86**(4), pp. 790–797.

[31] Phares, D. J., Smedley, G. T., and Flagan, R. C., 2000, "The Wall Shear Stress Produced by the Normal Impingement of a Jet on a Flat Surface," J. Fluid Mech., **418**(1), pp. 351–375.

[32] Loureiro, J. B. R., and Freire, A. P. S., 2012, "Wall Shear Stress Measurements and Parametric Analysis of Impinging Wall Jets," Int. J. Heat Mass Transfer, **55**(23–24), pp. 6400–6409.

[33] Ponce, P., Marcelli, D., Scholz, C., Wehmeyer, W., Gonçalves, P., Grassmann, A., Brand, K., and Canaud, B., 2014, "Does the Extracorporeal Blood Flow Affect Survival of the Arteriovenous Vascular Access?," Hemodialysis Int., **19**(2), pp. 314–322.

[34] Patard, J.-J., Bensalah, K., Lucas, A., Rodriguez, A., Manunta, A., Rivalan, J., Pogamp, P. L., Lobel, B., and Guillé, F., 2002, "Management of Vascular Access for Hemodialysis After Successful Kidney Transplantation," Scand. J. Urol. Nephrol., **36**(5), pp. 373–376.

[35] Glashan, R. W., and Walker, F., 1968, "A Histological Examination of Veins Used in Artificial Arteriovenous ('Quinton/Scribner') Shunts," Br. J. Surg., **55**(3), pp. 189–193.

[36] Rodrigues, L. T., Pengloan, J., Baudin, S., Testou, D., Abaza, M., Dahdah, G., Mouton, A., and Blanchard, D., 2000, "Treatment of Stenosis and Thrombosis in Haemodialysis Fistulas and Grafts by Interventional Radiology," Nephrol., Dial., Transplant., **15**(12), pp. 2029–2036.

[37] Reidy, M. A., and Schwartz, S. M., 1981, "Endothelial Regeneration. III. Time Course of Intimal Changes After Small Defined Injury to Rat Aortic Endothelium," Lab. Invest., **44**(4), pp. 301–308.

[38] Fingerle, J., Au, T. Y. P., Clowes, A. W., and Reidy, M. A., 1990, "Intimal Lesion Formation in Rat Carotid Arteries After Endothelial Denudation in Absence of Medial Injury," Arterioscler., Thromb., Vasc. Biol., **10**(6), pp. 1082–1087.